文章编号: 1001-9014(2018)05-0518-05

DOI: 10.11972/j.issn.1001-9014.2018.05.002

Preparation of large area and high performance flexible GaInP/GaAs/InGaAs tandem solar cells

ZHANG Meng-Yan[1,2], GUO Zhen[3], SUN Li-Jie[2*], CHEN Jie[2]

(1. Department of electronic engineering, Institute of information science and technology, East China Normal University, Shanghai 200241, China;
2. State Key Laboratory of space power technology, Shanghai Institute of Space Power Sources, Shanghai 200245, China;
3. Academy of military science of Chinese PLA, Beijing 100141, China)

Abstract: Flexible high-efficiency III-V multijunction solar cells are being developed for use in unmanned Aerial Vehicles (UAVs), wearable devices and space applications. The solar cell epitaxial layers are grown on GaAs substrate by metalorganic chemical vapor deposition (MOCVD) and then are transferred to flexible substrates by cold-bonding and epitaxial lift-off process (ELO). Through the design of ELO apparatus and a large number of experiments on the optimal parameter, GaAs solar cell structure can be effectively separated from 4-inch GaAs wafer without defects and degradation in performance. Recently, 30 cm^2 large area flexible GaInP/GaAs/InGaAs 3-junciton solar cells on 50 μm polyimide film achieved a 1-sun, AM0 conversion efficiency of 31.5% with an open-circuit-voltage of 3.01 V, a short-circuit current-density of 16.8 mA/cm^2, and a fill factor of 0.845. By using the very light PI substrate, the unit weight of the solar cell is only 168.5 g/m^2 and the specific power is up to 2 530 W/kg.

Key words: solar cells, flexible and high-efficiency, epitaxial lift-off, GaAs
PACS: 81.15.Gh, 84.60.Jt

大面积、高性能柔性 GaInP/GaAs/InGaAs 叠层太阳电池的制备

张梦炎[1,2], 郭 振[3], 孙利杰[2*], 陈 杰[2]

(1. 华东师范大学 信息科学技术学院电子工程系, 上海 200241;
2. 上海空间电源研究所 空间电源技术国家重点实验室, 上海 200245;
3. 中国人民解放军军事科学院, 北京 100141)

摘要: 柔性高效 III-V 族多结太阳电池正在被开发、应用于无人机、可穿戴设备和空间能源等领域. 采用 MOCVD 技术在 GaAs 衬底上制备太阳电池外延层, 之后通过低温键合和外延层剥离方法将外延层转移到柔性衬底上. 通过外延层剥离设备设计和大量参数优化实验, 实现了 GaAs 太阳电池结构从四英寸砷化镓晶圆上的有效分离, 且不产生缺陷并保持原有的性能. 近期, 在 50 μm 聚酰亚胺薄膜上制备的 30 cm^2 大面积柔性 GaInP/GaAs/InGaAs 三结太阳电池实现了 31.5% 的转换效率(AM0 光谱), 其中开路电压 3.01 V, 短路电流密度 16.8 mA/cm^2, 填充因子 0.845. 由于采用了轻质的聚酰亚胺材料, 所得到的柔性太阳电池面密度仅为 168.5 g/m^2, 比功率高达 2 530 W/kg.

关 键 词: 太阳电池; 柔性高效; 外延层剥离; 砷化镓

中图分类号: TN36 **文献标识码:** *A*

Received date: 2018-01-26, **revised date:** 2018-02-05 **收稿日期:** 2018-01-26, **修回日期:** 2018-02-05
Foundation items: Supported by the Shanghai Science and Technology Committee Rising-Star Program (14QB1402800)
Biography: ZHANG Meng-Yan(1984-), male, Zhuji of Zhejiang, doctoral candidate, Research area involves novel and high efficiency photovoltaic technology. E-mail: mengyanzhang@126.com
* **Corresponding author:** E-mail: sunlijielu@163.com

Introduction

GaInP/GaAs/Ge lattice matched triple-junction solar cells with high efficiency, high reliability and long life have become the main force of the space power supply [1,2]. However, it cannot be ignored that, despite the significant increase in the conversion efficiency, the weight of the substrate material seriously restricts the improvement of the specific power of the battery (W/kg). Another problem is that the Ge bottom cell absorbs approximately two times more low energy photons than are needed for current matching with the GaInP and GaAs subcells. It is well known that the Ge bottom junction would be replaced with a 1.0 eV $In_{0.3}Ga_{0.7}As$ junction that is lattice matched with the other junctions. Because of the 2% lattice mismatch between $In_{0.3}Ga_{0.7}As$ and other subcells, graded composition buffer layers (metamorphic) was adopted to avoid the dislocations. However, the remaining threading dislocations would significantly degrade any subsequently grown junctions with higher band gaps. By growing in an inverted configuration this degradation of the top junctions can be avoided [3].

Epitaxial lift-off (ELO), known as peeled film technology, was initially developed in the late 1980's [4]. With this technique III-V multijunction solar cells structures can be separated from their GaAs substrates using selective wet etching of a thin AlAs or Al_xGaAs ($x>0.6$) release layer. This technique allows for a significant cost reduction of the devices since the GaAs substrate can be reused after the lift-off process. The thin-film structures obtained by the ELO process can be cemented on arbitrary flat carriers for further processing [5-7]. As a result GaAs solar cell structure can be effectively separated from 4-inch GaAs wafer without defects and degradation in performance with a lateral etch rate of about 25 ~ 35 mm/h. However, subsequent processing these thin-film structures into actual ELO solar cells was found to be difficult because the epi-layers are very thin and fragile. Therefore, GaAs solar cells were transferred to flexible support substrate such as polyimide or metal foils by a bonding process before the ELO [8-10].

In this work, we demonstrate the application of the cold-bonding and epitaxial lift-off technique, as an effective substrate thinning method, for making ultra-light high-efficiency flexible triple junction InGaP/GaAs/InGaAs solar cells. Moreover, the growth technology of InGaAs subcell was further studied and large area (30 cm^2), high efficiency (31.5%, AM0) and high specific power (2 530 W/kg) flexible GaInP/GaAs/InGaAs tandem solar cells have been fabricated.

1 Experimental

In this study, the GaInP/GaAs/InGaAs inverted 3-junction cells was grown by Metalorganic Chemical Vapor Deposition and followed by cold-bonding and epitaxial lift-off. Figure 1 shows a typical process flow for flexible GaInP/GaAs/InGaAs tandem solar cells. The process starts with growth of inverted metamorphic (IMM) 3-junction GaInP/GaAs/InGaAs epitaxial layer, followed by the cold-bonding between epitaxial layer and PI thin film. After cold-bonding, epitaxial lift-off (ELO) process was conducted in order to transfer the solar cell's structure to the PI substrate. Finally, flexible solar cells can be prepared by rigid substrate fixation and traditional solar cell technology.

All metamorphic buffer and solar cells layers in this work have been grown by Metalorganic Chemical Vapor Deposition using an AIX2600-G3 reactor with 4-inch substrate. The n-GaAs substrates were used with a 7° offset from the (001) to (111) B plane and the carrier concentrations were $(1 \sim 4) \times 10^{18}$ cm^{-3}. The hydrid sources arsine and phosphine were used for the group-V-growth. Trimethylgallium at 7.5°C and ethyldimethylindium at 16°C were used as the group III precursors. SiH_4 was used as the dopant for n type doping of III-V compound epitaxial layers, while diethylzinc and CCl_4 were used as the p type dopants. The MOCVD growth conditions for each of these subcells were optimized to yield a high quality material with minimum defects and optimal electrical performance.

Both the epitaxial film of solar cells and the PI film were cleaned and passivated to a high quality of surface finish prior to subjecting the wafers to bonding. First, all the epitaxial subcells were cleaned by acetone, isopropanol and ethanol sequentially in an ultrasonic bath, then rinsed by deionized (DI) water, and finally dried with N_2. The polyimide (PI) thin films were first dipped in KOH solution and then cleaned in acetone and ethanol solutions to remove the pollutions of carbon and metal oxide. After that, a 50nm titanium film and then 300 nm gold film were deposited on the surface of PI and epitaxial layer by electron beam evaporation, respectively.

The bonding was carried out using Karl Suss SB6e wafer bonding equipment. The bonding parameters such as temperature, pressure and bonding time were carefully optimized to achieve high mechanical strength and low electrical resistance across the bonded interface. Scanning acoustic microscopy was used to determine the uniformity and quality of the bonded interface. After wafer bonding, the GaAs substrate was removed by using the ELO process. The etch solution concentration, temperature and ELO rate were carefully optimized.

2 Results and discussion

Figure 2 shows the schematic of inverted grown GaInP/GaAs/InGaAs 3J solar cells. The solar cell layers are grown in reverse order to be consistent with the ELO process. First, a 20 nm AlAs sacrificial layer was grown, and then GaInP top subcell, GaAs middle subcell and $In_{0.3}GaAs$ bottom subcell were grown in turn. GaInAlAs grade buffer structures were grown with a step-graded design between the GaAs and $In_{0.3}GaAs$ subcells. The grade consisted of eight 250 nm steps and a 800 nm tuning layer which was varied in composition. On top of the tuning layer, a final 200 nm $In_{0.3}GaAs$ layer lattice matched to the 1eV $In_{0.3}GaAs$ bottom cell layer was grown.

Figure 3 shows the characterization results for the epitaxial layer of GaInP/GaAs/InGaAs solar cell. High resolution X-ray diffraction in recent decades is the de-

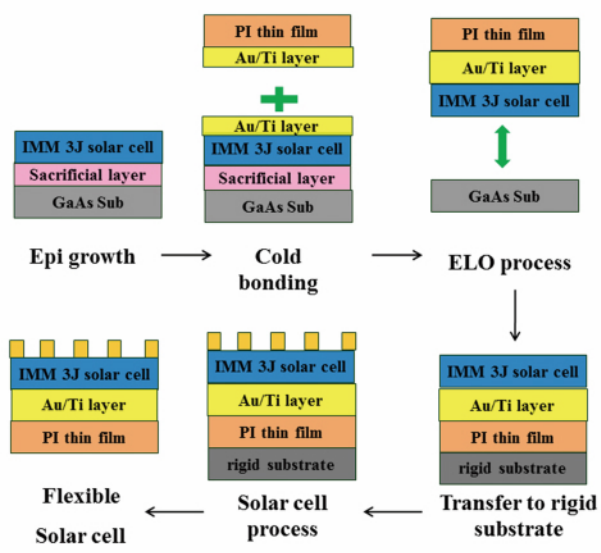

Fig. 1 The flexible GaInP/GaAs/InGaAs tandem solar cell process flow

图1 柔性 GaInP/GaAs/InGaAs 叠层太阳电池工艺流程图

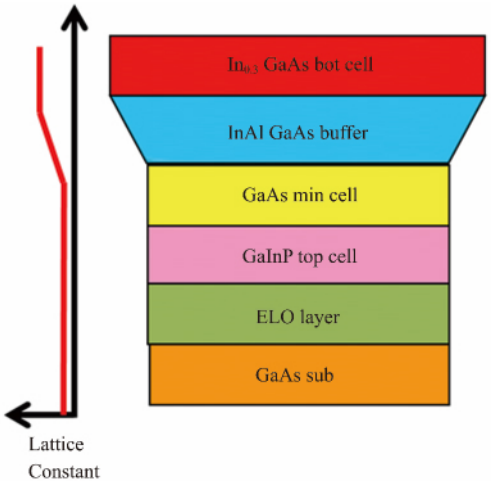

Fig. 2 Schematic of inverted grown GaInP/GaAs/InGaAs 3J solar cell

图2 反向生长的 GaInP/GaAs/InGaAs 三结太阳电池结构图

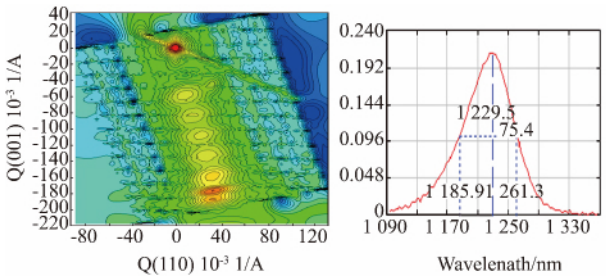

Fig. 3 Characterization of epitaxial layer of GaInP/GaAs/InGaAs solar cell: (a) XRD reciprocal space mapping diagram in (115) direction; (b) Photoluminescence spectroscopy at room temperature

图3 GaInP/GaAs/InGaAs 太阳电池外延层的测试表征(a)沿(115)晶向的 XRD 倒易空间图;(b)室温下的光致发光谱

velopment of a non-contact and nondestructive crystal quality detection technology, especially the reciprocal space map obtained by the three axis diffraction (RSM) can visually display the distribution of reciprocal lattice space scattering intensity. By analyzing the location and shape of reciprocal space map, we get directly the information about lattice integrity in defects, stress and strain, mosaic structure and interface matching condition in lattice. The stress state of the buffer layer and the subcells can be clearly seen by the HRXRD RSM. It is found that the GaInAlAs grade buffer layer is almost a complete relaxation state and relaxation degree calculated by the software is about 99% as figure 3(a) shown, which indicates that the dislocation caused by the lattice mismatch will be completely released into the buffer layer, making the InGaAs subcell have high material quality. In addition, it can be seen that the bottom subcell was a tensile state which is helpful to attain a high Voc.

Figure 3 (b) shows the PL (photoluminescence spectroscopy) of epitaxial layer of GaInP/GaAs/InGaAs solar cell at room temperature by using a 532 nm laser. Due to the band gap of the InGaAs material at the top is lower than other subcells, the PL signals of GaInP and GaAs cannot be detected since the luminescence below will be absorbed by the InGaAs. The PL peak of InGaAs is located at 1 229.5 nm, indicating the bandgap of InGaAs is about 1 eV (1 240 eV* nm/1 229.5 nm) and the Indium component is 29.9%, which is very consistent with the design value 30%. In addition, the FWHM (full width at half maximum) of the PL peak is only 75 nm showed that the $In_{0.3}GaAs$ material has very good material quality.

Figure 4 shows scanning acoustic microscopy test of the GaAs epitaxial wafer/PI film obtained by cold bonding process. The quality of bonding is mainly affected by the sample surface roughness, cleaning methods and bonding parameters. In addition, in order to avoid the influence of impurities, the whole bonding process is conducted in super clean room. After parameter optimization, we obtained a set of process parameters to achieve a large area uniform bonding: Chamber pressure: 2.00E-3 mbar; Bonding temperature: 250℃; Bonding pressure: 20 000N; Bonding time: 1 h. In order to achieve large area and high quality bonding, the cleaning process has been improved. It is can be seen that the hole or cavity in the bonding interface as shown in figure 4(a) were thoroughly removed as shown in figure 4(b).

Figure 5(a) shows schematic diagram of ELO process. The ELO epi-layer structure especially the sacrificial layer was optimized. In order to speed up the separation rate and shorten the process time, we mainly enhance the reaction gas escape rate by apply external forces and control the stress by our design of the ELO apparatus. Figure 5(b) shows the photo of flexible 3-junction InGaP/GaAs/InGaAs solar cell epitaxial layer on PI substrate obtained by bonding and ELO process. It can be seen that the surface of the sample is very bright and uniform, without defects such as peeling off, bubbles or cracks, indicating that the transfer process of the epitaxial layer has a high quality.

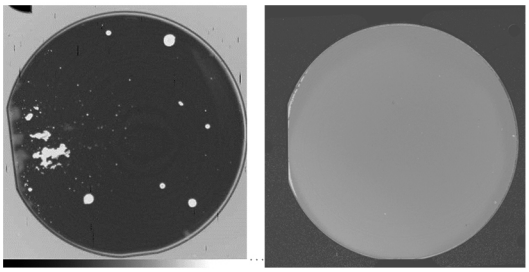

(a) (b)

Fig. 4 Scanning acoustic microscopy test of the GaAs epitaxial wafer/PI film obtained by cold bonding process (a) before cleaning optimization and (b) after cleaning optimization

图 4 GaAs 外延片与 PI 薄膜低温键合后的超声扫描测试结果(a) 样品清洗工艺优化前,(b) 样品清洗工艺优化后

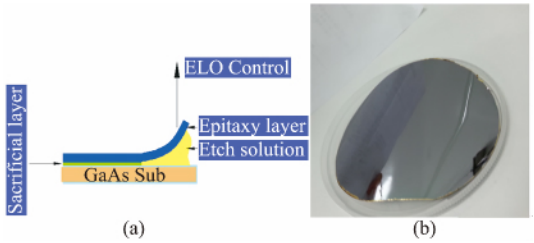

(a) (b)

Fig. 5 (a) Schematic diagram of ELO process and (b) the photo of flexible InGaP/GaAs/InGaAs solar cell epitaxial layer on PI substrate

图 5 外延层剥离过程示意图(a) 和制备到 PI 衬底上的柔性 InGaP/GaAs/InGaAs 太阳电池外延层照片

The 4-inch flexible InGaP/GaAs/InGaAs solar cell as shown in Fig. 6 can be obtained by traditional device process such as photo-lithography, development, metal deposition, ARC (Antireflection coating), etc. Depending on the application requirements, the flexible solar cells can be cut into different sizes by dicing machine and Fig. 6(b) shows the largest 4 × 8 cm^2 size (lack of two triangles on the edge, the real area is 30 cm^2) flexible InGaP/GaAs/InGaAs solar cell.

Figure 7 shows the result of the photovoltaic *I-V* characteristics of the 30 cm^2 flexible InGaP/GaAs/InGaAs solar cells with an open-circuit-voltage of 3.01 V, a short-circuit current-density of 16.8 mA/cm^2, a fill factor of 0.845 and AM0 conversion efficiency of 31.5%. The greatest improvement comes from the high Voc of the bottom subcell. Based our previous work, similar single-junction devices indicated that approximately 1.45 V comes from the 1.9 eV GaInP top junction, 1.03 V from the 1.424 eV GaAs middle junction. Therefore, the bottom $In_{0.3}GaAs$ subcell contributes about 0.53 V of open circuit voltage. Compared with the previous 0.48 V, it has been increased about 50 mV due to the tensile state in bottom subcell and the high material quality as Fig. 3 shown. By using the very light PI substrate, the unit weight of the solar cell is only 168.5 g/m^2 as shown in table 1. Thus, the specific power of flexible InGaP/GaAs/InGaAs solar cells is up to 2 530 W/kg, which is very suitable for application in unmanned Aerial Vehicles (UAVs), wearable devices and other space solar cell arrays with high demand for light and flexible thin film solar cells.

Table 1 Weight composition of each part of the flexible 3J solar cells

表 1 柔性三结太阳电池各组成部分的重量

Component	PI Substrate	Epitaxial layer	Bonding metal	ARC and grid electrode	The solar cell
Unit weight (g/m^2)	70.0	73.1	20.6	4.8	168.5

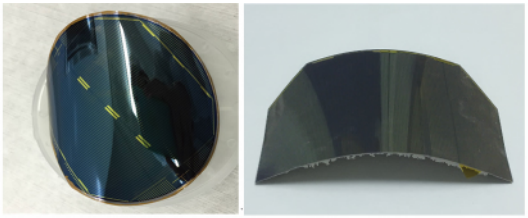

(a) (b)

Fig. 6 The flexible InGaP/GaAs/InGaAs solar cells (a) 4-inch wafer size, (b) 4cm × 8cm size

图 6 柔性 InGaP/GaAs/InGaAs 太阳电池(a) 四英寸晶圆尺寸 (b) 4cm × 8cm 尺寸

The external quantum efficiency (EQE) of all three junctions was shown in figure 8. It is obvious that the peak EQE of the GaInP and GaAs subcells is close to 90%, while the peak EQE of the $In_{0.3}GaAs$ subcell is also more than 80%. In general, the QE curve of InGaAs subcell is downward sloping from 900 nm to 1 250 nm, but it is relatively flat here, which may be related to the photons reflection effect of the back metal (for cold bonding). Other workers have reported enhanced solar cell performance by including a DBR stack in the buffer layers of GaAs solar cells to promote photon recycling [11].

To further improve the efficiency, the ARC needs to be optimized to reduce the average reflectivity from 300 nm to 1 300 nm. In addition, it is necessary to point out that, the flexible GaInP/GaAs/InGaAs solar cells can't be annealed at high temperature above 250℃ due to the limitation of flexible thermoplastic substrate. Therefore, new flexible substrates or low temperature annealing electrode materials are now in progress in order to further lower the contact resistance of the electrode, enhance the fill factor up to 0.86 and increase the efficiency exceeding 32%.

3 Summary

Flexible high-efficiency III-V multijunction solar cells are being developed by using the cold-bonding and epitaxial lift-off process (ELO). Through the design of ELO apparatus and a large number of experiments on the optimal parameter, GaAs solar cell structure can be effectively separated from 4-inch GaAs wafer without defects and degradation in performance. Recently, high quality 1.0 eV $In_{0.3}GaAs$ subcell and GaInP/GaAs/$In_{0.3}$

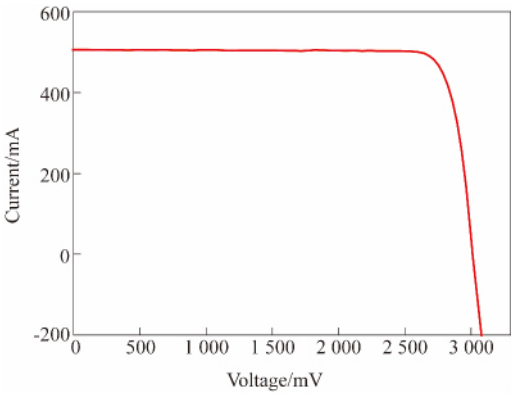

Fig. 7 Photovoltaic *I*-*V* characteristics of flexible InGaP/GaAs/InGaAs solar cell

图7 柔性 InGaP/GaAs/InGaAs **太阳电池的光照** *I*-*V* **曲线**

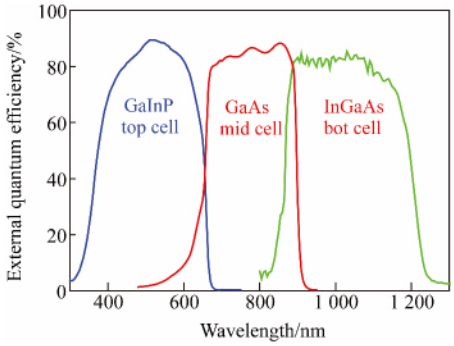

Fig. 8 External quantum efficiency of flexible InGaP/GaAs/InGaAs solar cell

图8 柔性 InGaP/GaAs/InGaAs **太阳电池的外量子效率**

GaAs epitaxial layers have been fabricated. Combined with flexible thin film solar cells preparation process, 30 cm^2 large area flexible GaInP/GaAs/InGaAs 3-junciton solar cells on 50 μm polyimide film achieved a 1-sun, AM0 conversion efficiency of 31.5% with an open-circuit-voltage of 3.01 V, a short-circuit current-density of 16.8 mA/cm^2, and a fill factor of 0.845. By using the very light PI substrate, the unit weight of the solar cell is only 168.5 g/m^2 and the specific power is up to 2 530 W/kg.

References

[1] Sato S I, Miyamoto H, Imaizumi M, *et al*. Degradation modeling of InGaP/GaAs/Ge triple-junction solar cells irradiated with various-energy protons [J]. *Solar Energy Materials & Solar Cells*, 2009, **93**(6): 768-773.

[2] Lan D, Green M A. Limiting efficiencies of GaInP/GaAs/Ge up-conversion systems: Addressing the issue of radiative coupling [J]. *Applied Physics Letters*, 2016, **109**(12): 42.

[3] Geisz J F, Kurtz S, Wanlass M W, *et al*. High-Efficiency GaInP/GaAs/InGaAs Triple-Junction Solar Cells Grown Inverted with a Metamorphic Bottom Junction [J]. *Applied Physics Letters*, 2007, **91**(2): 760.

[4] Yablonovitch E, Gmitter T, Harbison J P, *et al*. Extreme selectivity in the lift - off of epitaxial GaAs films [J]. *Applied Physics Letters*, 1987, **51**(26): 2222-2224.

[5] Cheng C W, Shiu K T, Li N, *et al*. Epitaxial lift-off process for gallium arsenide substrate reuse and flexible electronics [J]. *Nat Commun*, 2013, **4**: 1577.

[6] Schermer J J, Mulder P, Bauhuis G J, *et al*. Epitaxial Lift-Off for large area thin film III/V devices [J]. *physica status solidi* (*a*), 2005, **202**(4): 501-508.

[7] Wu F-L, Ou S-L, Horng R-H, *et al*. Improvement in separation rate of epitaxial lift-off by hydrophilic solvent for GaAs solar cell applications [J]. *Solar Energy Materials and Solar Cells*, 2014, **122**: 233-240.

[8] Moon S, Kim K, Kim Y, *et al*. Highly efficient single-junction GaAs thin-film solar cell on flexible substrate [J]. *Sci Rep*, 2016, **6**: 30107.

[9] Nam J, Lee Y, Choi W, *et al*. Transfer Printed Flexible and Stretchable Thin Film Solar Cells Using a Water-Soluble Sacrificial Layer [J]. *Advanced Energy Materials*, 2016, **6**(21): 1601269.

[10] Ward J S, Remo T, Horowitz K, *et al*. Techno-economic analysis of three different substrate removal and reuse strategies for III-V solar cells [J]. *Progress in Photovoltaics: Research and Applications*, 2016, **24**(9): 1284-1292.

[11] Johnson D C, Ballard I, Barnham K W J, *et al*. Advances in Bragg stack quantum well solar cells [J]. *Solar Energy Materials & Solar Cells*, 2005, **87**(1): 169-179.

(上接第 517 页)

[26] Lin T-T, Ohtani K, Ohno H. Thermally Activated Longitudinal Optical Phonon Scattering of a 3.8 THz GaAs Quantum Cascade Laser [J]. *Appl. Phys. Express*, 2009, **2**: 022102-1-022102-3.

[27] Matyas A, Chashmahcharagh R, Kovacs I, *et al*. Improved terahertz quantum cascade laser with variable height barriers [J]. J. Appl. Phys. 2012, **111**: 103106-1-103106-6.

[28] Lin T-T, Hirayama H. Variable Barrier Height AlGaAs/GaAs Quantum Cascade Laser Operating at 3.7 THz [J]. *Phys. Status Solidi A*, 2018, **215**: 1700424.

[29] Lin T-T, Ying L, Hirayama H. Threshold Current Density Reduction by Utilizing High-Al-Composition Barriers in 3.7 THz GaAs/Al*x*Ga$_1$-*x*As Quantum Cascade Lasers [J]. *Appl. Phys. Express*, 2011, **5**: 012101-1-012101-3.

[30] Luo H, Laframboise S R, Wasilewski Z R, *et al*. Terahertz quantum-cascade lasers based on a three-well active module [J]. *Appl. Phys. Lett*. 2007, **90**: 041112-1-041112-3.

[31] Kumar S, Hu Q, Reno J R, 186 K operation of terahertz quantum-cascade lasers based on a diagonal design [J]. *Appl. Phys. Lett*. 2009, 94: 131105-1-131105-3.

[32] Lin T-T, Hirayama H. Improvement of operation temperature in GaAs/AlGaAs THz - QCLs by utilizing high Al composition barrier [J]. *Phys. Status Solidi C*, 2013, **10**: 1430-1433.